HHS Public Access

Author manuscript

Brain Stimul. Author manuscript; available in PMC 2023 March 01.

Published in final edited form as:

Brain Stimul. 2022 ; 15(2): 316–325. doi:10.1016/j.brs.2022.01.007.

Large-Scale EEG Neural Network Changes in Response to Therapeutic TMS

Michael C. Gold[1,2], **Shiwen Yuan**[1,2], **Eric Tirrell**[1], **E. Frances Kronenberg**[1], **Jee Won D. Kang**[1], **Lauren Hindley**[1], **Mohamed Sherif**[2,3], **Joshua C. Brown**[1,2], **Linda L. Carpenter**[1,2]

[1]Butler Hospital TMS Clinic and Neuromodulation Research Facility, Providence RI

[2]Department of Psychiatry and Human Behavior, Alpert Medical School, Brown University

[3]Lifespan Physician Group, Rhode Island Hospital, Providence RI

Abstract

Background: Transcranial magnetic stimulation (TMS) is an effective therapy for patients with treatment-resistant depression. TMS likely induces functional connectivity changes in aberrant circuits implicated in depression. Electroencephalography (EEG) “microstates” are topographies hypothesized to represent large-scale resting networks. Canonical microstates have recently been proposed as markers for major depressive disorder (MDD), but it is not known if or how they change following TMS.

Methods: Resting EEG was obtained from 49 MDD patients at baseline and following six weeks of daily TMS. Polarity-insensitive modified k-means clustering was used to segment EEGs into constituent microstates. Microstates were localized via sLORETA. Repeated-measures mixed models tested for within-subject differences over time and t-tests compared microstate features between TMS responder and non-responder groups.

Results: Six microstates (MS-1 - MS-6) were identified from all available EEG data. Clinical response to TMS was associated with increases in features of MS-2, along with decreased metrics

Corresponding Author: Dr.Linda Carpenter, linda_carpenter_md@brown.edu, 345 Blackstone Blvd, Providence, RI 02906.

Author Contributions (CRediT roles)

MCG: Conceptualization; Data curation; Formal analysis; Investigation; Methodology; Project administration; Visualization; Writing - original draft; Writing - review & editing.

SY: Conceptualization; Investigation; Data curation; Writing - review & editing.

ET: Data curation; Project administration; Resources; Writing - review & editing.

EFK: Methodology; Investigation; Data curation.

JDK: Investigation; Data curation; Writing - review & editing.

LH: Investigation; Data curation.

MS: Conceptualization; Methodology; Writing - review & editing.

JCB: Conceptualization; Writing - review & editing

LLC: Conceptualization; Formal analysis; Funding acquisition; Investigation; Methodology; Supervision; Writing - original draft; Writing - review & editing.

“Microstates.”

CREDIT Authorship Contribution Statement

All authors approved the final version of the manuscript, and participated in its conceptualization. Statistical analyses and computational analyses were carried out by MG, and supervised by LC, JB, and MS. The manuscript was drafted by MG, LC, JB and SY with critical review and additional input by all authors. ET, JW, EF, LH, participated in data collection and data processing.

of MS-3. Nonresponders showed no significant changes in any microstate. Change in occurrence and coverage of both MS-2 (increased) and MS-3 (decreased) correlated with symptom change magnitude over the course of TMS treatment.

Conclusions: We identified EEG microstates associated with clinical improvement following a course of TMS therapy. Results suggest selective modulation of resting networks observable by EEG, which is inexpensive and easily acquired in the clinic setting.

Keywords

TMS; EEG; microstates; MDD; neuromodulation

Introduction

Repetitive Transcranial Magnetic Stimulation (rTMS or simply “TMS”) is an effective therapy for treatment-resistant major depressive disorder (MDD). While its putative mechanism of action is not known, TMS modulates dysfunctional global networks underlying depression symptoms (1). Imaging studies have shown TMS activates distal nodes of specific functional networks, and in turn, elicits sustained connectivity changes correlated with clinical improvement (2). In addition to global effects, the repetitive pulses of TMS entrain stimulation-site cortical oscillations to the frequency of stimulation (3). These local dynamics also appear relevant to TMS therapeutic mechanism of action, as the proximity of an individual’s endogenous peak alpha frequency to the stimulation frequency applied during TMS therapy is associated with better treatment response (4) (5).

While the efficacy of TMS therapy is robust for a population that has not benefitted from trials of standard antidepressant medications, only about 50% of patients who undergo TMS will see improvement from a six-week daily course (6). These outcome disparities likely reflect a heterogenous etiology within the broad depression diagnosis. Functional magnetic resonance imaging (fMRI) has quantified this heterogeneity as differences in resting state functional connectivity (7), but recent work has shown electroencephalographic (EEG) scalp recordings can accurately delineate depression subtypes (8). Particularly in light of its relatively low cost, portability, and ease of use compared to fMRI, the use of EEG to identify intra-diagnosis differences in clinical samples undergoing TMS holds promise for improving results via personalized, targeted protocols and predicting treatment outcomes (9) (10).

Other recent work has characterized large-scale network dynamics altered in depression using EEG microstates (11). EEG microstates are semi-stable, transient voltage topographies that are frequently recurring in resting-state EEG. Individual consistently-recurring microstate voltage topographies are likely generated by repeated co-activation of connected brain regions, generating a consistently recurring and temporarily stable pattern of positive and negative voltages which can be detected at the scalp. Microstates last approximately 80ms before shifting to another temporarily stable pattern. A set of four “canonical” microstates (A-D) exist in almost all subjects, and these states are believed to represent the synchronous activity of large-scale network nodes (12). In studies of disease abnormalities, microstates offer the ability to capture cortical activity from the entire EEG montage in a computationally optimized method. While the four canonical prototypes commonly appear

in awake EEG, microstates can be clustered from the EEG recordings in any given study without *a priori* assumptions about the number of prototypical maps to be selected; rather, goodness-of-fit measures determine the optimal number of topographies in each dataset. This data-driven approach is advantageous for studies of brain disorders in which aberrant (i.e. non-canonical) networks may manifest clinical symptoms.

Abnormalities in the temporal dynamics of resting state cortical activity have been associated with specific EEG microstate findings in neuropsychiatric disorders such as schizophrenia, delirium, and multiple sclerosis (see review by (12)). Recently, Murphy and colleagues (11) identified both state and trait microstates characterizing MDD, and a report by Yan et al. (13) identifies microstate changes associated with Selective Serotonin Reuptake Inhibitor (SSRI) - mediated MDD improvement. Additionally, certain microstates predicted clinical response in patients with treatment resistant depression who underwent both magnetic seizure therapy (MST) and electroconvulsive therapy (ECT) (14). Data describing effects of TMS on microstates are limited to one study of patients with schizophrenia (15); changes in two microstates' durations were interpreted as normalization of networks associated with symptoms. We investigated microstates in treatment-resistant MDD patients undergoing a standard, six-week rTMS therapy course in a naturalistic setting to evaluate possible microstate changes associated with rTMS and their relationship to treatment outcomes. While we considered these analyses to be largely exploratory, our hypotheses were based on the few published microstates findings in depression and following brain stimulation treatments. We anticipated that microstates would selectively change in patients who experienced improvement in depressive symptoms, reflective of large-scale functional network modulation previously shown to be involved in MDD pathology and TMS mechanism of action.

Methods

Subjects

All subjects had a primary diagnosis of MDD confirmed through clinical interview by experienced psychiatrists applying diagnostic criteria from the *Diagnostic and Statistical Manual of Mental Disorders* (5th ed.) (16). Subjects received a standard course of TMS therapy at the Butler Hospital TMS Clinic. The research protocol for collection of EEG data was approved by the Butler Hospital Institutional Review Board. All subjects provided informed consent prior to any procedures being performed. Subjects continued to receive previously prescribed psychotropic medications during their course of TMS therapy, consistent with routine standard of care. Butler TMS Clinic patients undergo routine medical clearance before receiving TMS treatment and are assessed with standardized self-report depression assessment scales at pre-treatment baseline, and after every 5 TMS sessions (17) (18).

Clinical Outcome

Clinical outcome was based upon change (from pre-treatment baseline to endpoint, represented as percent relative to baseline) of total score on the 30-item Inventory of Depressive Symptomatology, Self-Report scale (IDS-SR) (19). Categorical clinical

"response" was defined as a decrease of ≥50% in total IDS-SR score at the time of the post-TMS EEG. This outcome measure is widely used in the clinical and research fields surrounding TMS therapy for depression. For correlation and regression analyses, IDS-SR change over treatment was calculated as a baseline-adjusted endpoint score. Antidepressant response can be nonlinear, as more severely depressed patients show a greater percent change at endpoint. As a more appropriate measure of change in symptom severity for modeling purposes, we applied a six knot, restricted cubic spline regression of the post-TMS IDS-SR score using baseline IDS-SR (20). The cubic spline regression approach was used to specifically quantify the correlation of significant changes in microstate metrics and antidepressant changes. Regressing out the baseline score from the endpoint measure with this method creates a transformed value to more rigorously assess the relationship of neuroimaging changes with antidepressant effect. The selection of knots was based on similar prior investigations (21, 22).

TMS Therapy Course

Patients underwent a series of once-daily (weekdays) TMS treatment sessions on Neurostar (Neuronetics Inc., Malvern, PA) TMS devices with figure-8 coils incorporating an iron core. The course of treatment was delivered per Butler TMS Clinic's standard of care, and typically included protocols for stimulation at 10 Hz or 5 Hz over the left dorsolateral prefrontal cortex (DLPFC) at 120% intensity, relative to left-sided resting motor threshold, with a total of 3000 pulses per session. In cases of poor tolerability, some patients (n=4) were switched to unilateral 1Hz stimulation sessions (1800 pulses per session) over the right DLPFC. A typical course of TMS therapy includes 30 sessions over 6 weeks followed by 6 additional sessions in a taper schedule, but a small minority of patients received fewer or more sessions in their course of treatment, based on clinical response and other factors.

EEG Recording and Processing

Sixty-four channel EEG data were recorded at 2000Hz or 2048Hz sampling rate with CPz electrode reference during the first session of each patient's course ("pre") and again 6 weeks later at the end of the course ("post") with the ANT TMS-compatible EEG system (Advanced Neuro Technology [ANT]; Enschede, the Netherlands). At each timepoint, five minutes of eyes-closed resting EEG was acquired. Offline preprocessing was conducted in the EEGLAB toolbox (v2020.0) (23) for MATLAB (2019b, The MathWorks Inc). The two mastoid channels were presumed to contain no neural data and removed, leaving 61 channels for analysis. Data was down sampled to 200Hz with the EEGLAB *pop_resample* antialiasing filter using a cutoff of 160Hz and transition bandwidth of 80Hz, high-pass filtered at 1Hz, and cleaned of large artifactual segments and noise by EEGLAB's *clean_rawdata*. Bad channels were rejected and spherical spline interpolated (24). Data was re-referenced to common average and 60Hz line noise was removed using Zapline (25). The down-sampled and cleaned data was then submitted to AMICA (26) for independent component analysis. Components were localized using DIPFIT3 (v3.4) by fitting single equivalent current dipoles to a template head model (27). Neural components were identified by two criteria: components labeled "brain" by ICLabel (v1.2.3) (28), and components localized inside the brain with a residual variance < 15% (29). Non-neural, artifactual

components were removed before further analysis. Prior to Microstate Analysis, the pre-processed recordings were low-pass filtered at 30Hz.

Microstate Clustering

While the sample selected for analysis in this study reflected just those patients who had EEG data collected both at baseline and following their most recent course of TMS treatments, a larger dataset comprising all available resting EEG data was used for clustering with the Microstate Analysis Toolbox (v1.0) (30) implemented in EEGLAB. Recordings from both pre-treatment and post-treatment were clustered simultaneously to ensure identification of shared microstate prototypes and to improve odds of selecting prototypes relevant to TMS. Additionally, clustering across sessions and conditions, rather than separately for each, has been shown to reduce within-subject error and ensure test-retest reliability (31).

Clustering was calculated by a polarity-insensitive modified k-means algorithm (32). The k-range was set from 2 to 8, with 50 random start repetitions for each k to improve replicability. The number of prototype maps was determined as the optimization value of both the Global Explained Variance (GEV) and Cross-Validation Criteria over the k-range. The Krzanowski-Lai (KL) criterion (33) is an additional, commonly-used metric to select the number of microstates; however, KL is not a polarity insensitive measure and, accordingly, was not considered in this analysis.

After choosing the number of states and their corresponding voltage maps, the prototype maps were backfit to the entire duration of recordings for the study sample (n=49). Each EEG sample was labeled as a microstate in a winner-take-all approach, segmenting EEG into constituent microstates. The minimum microstate segment duration was set to 30ms. Three variables of interest were extracted from the microstate label time series: occurrence, coverage, and duration. Occurrence is the frequency of microstate appearance in states/second; coverage measures the proportion of the total recording dominated by a given microstate; and duration is the average length, in milliseconds, a microstate class remains active when it appears.

Source Analysis

Microstates were source localized using the Brainstorm Toolbox for MATLAB (34). For subjects included in formal analysis, individual EEG data was extracted and concatenated by microstate. These concatenated-microstate recordings were imported to Brainstorm. Standard 10–20 electrode locations were co-registered to an ICBM25 template head MRI, and a boundary element model forward solution was calculated using OpenMEEG (35). Standardized low-resolution electromagnetic tomography (sLORETA) localized scalp signal to cortically constrained (normal to cortex) source space (36). For each subject, individual microstate source activations were averaged across time. For each microstate, subject-average source maps were z-scored, rectified, and group averaged. Group-averaged maps were thresholded to activations above 95^{th} percentile, as suggested in fMRI conjunction analysis (37). Source analysis was only performed on pre-TMS recordings due to computational constraints.

Statistics

Formal analysis was conducted in MATLAB, SPSS 26 (IBM), and RStudio (v1.4.1106). Pearson correlations and independent samples t-tests were used to evaluate microstate features relative to baseline depression severity and demographic features. Repeated-measures analyses of variance tested for differences in microstate metrics over time between responder and non-responder groups, utilizing time as a within-subjects factor and responder status as between-subjects factor. Thus, a main effect of time for all subjects and an interaction effect of responder status were evaluated with significance thresholds adjusted for testing the 3 features within each microstate domain, i.e, alpha=0.017. When a significant effect of response group effect was found, sensitivity analyses were run with age and sex included in the models. Paired Student's *t*-tests (two-tailed) compared Pre versus Post microstate means in the overall sample and in each treatment outcome group. To be consistent with the methods described in other microstates analyses, p-values for the paired t-tests were Bonferroni-corrected for the number of microstates tested within each response group ($p = 0.05/6 = .0083$ for significance). Effect size for paired-sample tests were calculated using Cohen's *d*. To evaluate treatment-predictive characteristics of microstates, Pearson correlations tested the association between changes in microstate metrics with changes in depression severity (calculated as IDS-SR % change from baseline to treatment endpoint). Significance thresholds for microstate correlations with baseline features and IDS-SR change values were uncorrected due to their exploratory nature. Sensitivity analyses were conducted by inclusion of age and sex as covariates in statistical models.

Results

Clinical Outcomes

Patient (n=49) demographics and clinical history are presented in Table 1. Depression outcomes assessed at the timepoint closest to the "post" EEG were used to provide an accurate measure of clinical changes between the two recording sessions. Patients saw a significant reduction in depressive symptoms over the course of TMS therapy (IDS-SR mean±SD change: −23.1±15, $t = -10.8$, $p < 0.0001$, $d = 1.6$), as expected from open-label trials. At the time of post-EEG data acquisition, 21/49 (43%) met criteria for categorical response to TMS. Responders and non-responders did not significantly differ in any baseline clinical characteristics.

Microstate Analysis

Six microstates were identified from clustering 175 recordings (Figure 1). The 175 recordings included both Pre-TMS (n=110) and Post-TMS (n=65) phases of EEG data collection, representing 98 unique MDD patients treated in our TMS clinic. Of the 65 patients with post-treatment recordings, 61 had corresponding pre-treatment recordings. The 61 matched Pre- and Post-TMS recordings comprised 52 unique subjects, as some subjects received multiple TMS treatment courses. Of these, EEG from the most recent course of TMS treatment was utilized for formal analysis of microstate change related to clinical response. Finally, 3 patients had incomplete clinical outcomes at the time of our current analysis and were removed from the dataset, leaving a final sample of 49 for formal analysis of microstate change associated with TMS.

The six microstates explained 76.5% of global variance and had a cross-validation score of 0.3 across all recordings (Supplemental Figure 1). The GEVs of individual microstates (MS1-MS6) were, in order, 0.31, 0.19, 0.095, 0.093, 0.064, 0.051. The four common microstates appear to be represented in this set, as expected. MS-1 corresponds to canonical C, MS-3 to D, MS-4 to B, and MS-5 to A. MS-2 appears to similarly be a derivative of canonical state C. We used this visual similarity as a basis for comparison to prior relevant microstate investigations (Supplemental Figure 2).

Microstate Relationship to Baseline Characteristics

At baseline, pre-treatment depression severity was correlated with the MS-1 coverage ($r = 0.34$, $p = 0.02$) and occurrence ($r = 0.33$, $p = 0.02$). No other microstate metric (coverage, occurrence, duration) was related to self-rated depression scores. Neither age nor sex was significantly related to any of the microstate metrics at baseline.

Microstates Changes Associated with TMS Therapy

Results of the repeated measures mixed models revealed significant ($p < 0.015$ corrected threshold) main effects of time for MS-2 (occurrence $p = 0.005$, $F = 8.74$; duration $p = 0.014$, $F = 6.51$; coverage $p = 0.006$, $F = 8.36$), and MS-3 (occurrence $p = 0.004$, $F = 9.15$; coverage $p = 0.006$, $F = 8.38$) reflecting increases in MS-2 and decreases in MS-3 (see supplemental Table 2). When pre-TMS vs post-TMS changes were analyzed with paired t-tests and the more stringent correction for multiple comparisons was applied, none of the mean changes for the pooled sample (n=49) reached the significance threshold ($p < 0.008$) (see top row in Figures 2 and S2).

Microstate Changes Associated with Response to TMS Therapy

Motivated by prior work showing the responder-specific physiological effects of rTMS (1, 10, 38) and consistent with our hypothesis that TMS responders would display changes in microstate dynamics, we evaluated microstate changes within each response group (≥50% improvement IDS-SR = responder; Figure 2a,b).

Repeated-measures models showed responder status had a significant effect on MS-2 changes in occurrence ($F(1,47) = 6.38$, $p=0.015$, $p_{bonferroni} = 0.045$); this finding retained significance when age and sex were entered as covariates. TMS responders (n=21) had significantly increased occurrence (mean ± SD, pre: 2.29 ± 0.6; post: 2.79 ± 0.56, $p =.007$, $p_{bonferroni} = 0.042$, $d=0.67$) and coverage (pre: 0.17±0.05; post: 0.22 ± 0.07; $p = 0.006$, $p_{bonferroni} = 0.036$, $d = 0.68$) of MS-2 from pre- to post- treatment. By contrast, non-responders (n=28) showed no change in MS-2 occurrence ($p = 0.69$), coverage ($p = 0.48$), or duration ($p = 0.25$). Duration of MS2 among responders did not change significantly over the course treatment ($p = 0.023$, $p_{bonferroni} = 0.14$).

For MS-3, repeated measures models showed trend-level effects of responder status on changes in occurrence ($F(1,47) = 5.57$, $p = 0.023$; $p_{bonferroni} = 0.069$), duration ($F(1,47) = 5.86$, $p=.019$, $p_{bonferroni} =.057$), and coverage ($F(1,47) = 6.25$, $p = 0.016$, $p_{bonferroni} = 0.048$); p-values remained unchanged or were further reduced in sensitivity analyses with age and sex. Paired-t-tests revealed that among responders, MS-3 occurrence decreased (pre:

2.39 ± 0.69; post: 1.88 ± 0.74; p = 0.001, $p_{bonferroni}$ = 0.006, d = 0.87). MS-3 coverage similarly decreased for responders from baseline (0.18 ± 0.086) to endpoint (0.13 ± 0.058; p = 0.006, $p_{bonferroni}$ = 0.036, d=0.67). No significant change was seen in MS-3 duration among responders ($p_{bonferroni}$ = 0.156). Nonresponders did not have significant change in MS-3 occurrence (p = 0.64), coverage (p = 0.73), or duration (p = 0.86). Post-hoc tests indicated that the increase in MS-2 characteristics and decrease in MS-3 characteristics were significantly correlated (change in occurrence: r = −0.54, p < 0.0001; coverage: r = −0.48, p < 0.0001), suggesting a true reciprocal relationship.

For responders, paired-t-tests suggested MS-6 decreased in duration from pre-TMS (68 ± 4.7) to post-TMS (64 ± 5.8, p = 0.003, $p_{bonferroni}$ = 0.018, d = 0.73). Non-responders saw no change in MS-6 duration (p = 0.66). However, this responder interaction did not meet significance in the repeated measures model ($F_{(1,47)}$ = 3.12, p = 0.084, $p_{bonferroni}$ = 0.24). No other significant duration changes were observed (Supplemental Figure 3).

Microstates 1, 4, and 5 revealed no significant changes over the course of TMS treatment for either response group or nonresponse group.

After observing the responder-specific changes in MS-2 and MS-3, we evaluated the explicit relationship of microstate changes to degree of improvement in depression symptoms (Figure 3). Change between timepoints [post-pre] in each microstate metric (occurrence, coverage, duration) was examined in correlation tests with symptom change (IDS-SR endpoint score corrected for baseline, where more negative values represent a greater degree of depressive symptom reduction). Symptom improvement over the course of TMS was associated with increases in MS-2 occurrence (r = −0.44, p = 0.002, Figure 3a) and coverage (r = −0.39, p = 0.006, Figure 3b). Symptom improvement was also associated with a greater decrease in MS-3 occurrence (Pearson r = 0.35, p = 0.01, Figure 3c) and MS-3 coverage (r = 0.34, p = 0.02, Figure 3d). No significant associations were observed between changes in duration of MS-6 and clinical change. In total, 3 p-values (uncorrected) were generated for correlations with symptom improvement within each of the 3 microstates that showed significant changes (MS-2, MS-3, MS-6) in prior analyses; Bonferroni correction would decrease the significance threshold to p = 0.017 for these tests.

Localization of Modulated Microstate Networks

Microstates represent spatially stable topographies of neural signal. Multiple reports have linked the canonical microstates to certain functional networks in combined fMRI/EEG studies (39), and source localization of microstate EEG signal to cortex has been performed using various algorithms.

Microstates overlap in their neural generators while also retaining distinct network properties (40). In light of the observed reciprocal changes in MS-2 and MS-3 prominent among TMS responders, we visually compared their source localizations. MS-2 activated most strongly in the frontal/temporal poles, rostral anterior cingulate cortex, orbitofrontal cortex, and anterior insula. In contrast, MS-3 appears to represent activity in the posterior cingulate, motor/premotor areas, and parietal lobe. Microstates 1, 3, 4, and 5, appear grossly

similar to previous localizations of their analogous canonical microstates (Figure 4b and Supplemental Figure 4) (12).

Discussion

While TMS is an effective therapy, its antidepressant mechanisms of action remain uncertain. The heterogeneity in response to TMS suggests, at least in part, different underlying dysfunctional networks and subtypes of MDD are at play (7) (41). EEG-derived biomarkers hold promise to define depression endophenotypes that share common neurophysiological features and to improve patient outcomes via targeted treatment selection.

In this study we identified microstate networks that were dominant over time, i.e., in both pre- and post-treatment resting EEG data, then evaluated changes in these (six) microstates after a standard 6-week course of naturalistic TMS therapy in patients with MDD. We found differential changes in multiple microstates as a function of response to TMS therapy; two specific microstates (presented here as MS-2 and MS-3) significantly and reciprocally changed among responders. Consistent with other groups (e.g. (42)), we did not find baseline microstates to be associated with treatment outcomes. After a standard course of TMS, however, those who got better showed significant increases in the presence of MS-2 alongside significant decreases in MS-3. The robustness of these findings was also reflected by correlation analyses indicating the magnitude of changes in microstates 2 and 3 significantly correlated with degree of clinical improvement.

Microstates are believed to represent transient activations of global networks. While recent work on microstates in depression (11) was limited by use of prototype voltage maps to localize cortical signal to unconstrained source, we applied sLORETA localization to our recorded subject EEG data (see Figure 4 and Supplementary Figure 4) and observed distinct networks that changed in relation to clinical response to TMS. Previous fMRI/EEG work has attempted to translate the spatially imprecise microstate networks onto their underlying cortical sources. Canonical microstate C, which corresponds to our microstate 2, had BOLD activation in the dorsal anterior cingulate cortex (ACC), inferior frontal cortices, and right insula (39) (Fig 4a). These regions, along with our microstate 2 source localization, overlap favorably with the positive affective “reward” circuit, involving the orbitofrontal cortex, the anterior and inferior prefrontal cortex, and ACC (43). Our finding suggests that in TMS responders, this reward network may be activated more often and for a greater proportion of time, perhaps reflecting changes underlying improvement in anhedonia. However, we did not directly test the relationship between specific symptoms and microstate networks, and so these interpretations are merely speculative, constituting a future direction in this line of investigation.

In contrast, microstate 3 was decreased in coverage and occurrence after effective TMS (Figure 4b). This microstate corresponds to canonical microstate D, both of which activate dorsal and ventral frontal and parietal cortical areas (12, 39) subserving depression networks of attention and cognitive control (43). Interestingly, while depression is commonly associated hypoconnectivity of the cognitive control networks (44), other evidence suggests

that some depressed patients indeed have hyperconnectivity in this network, which has been suggested to contribute to ruminative thoughts, and is further reflected in the positive correlations between this network and the default mode network (43). We again emphasize that our speculations require direct testing correlating symptoms with network changes, and future work would be complemented well with functional imaging to combine spatial and temporal precision in elucidating the EEG microstate correlates of depression symptom subtypes (45).

As depression subtypes have been explained by functional connectivity differences (7) and stimulation site connectivity may predict TMS treatment outcomes (46), the question of network changes induced by treatment is particularly important to the mechanism of action of TMS therapy. Our results appear generally consistent with prior work showing that connectivity between the dorsolateral prefrontal cortex (stimulation site) and subgenual ACC is relevant to TMS treatment outcome (47) and that frontoparietal networks play a role in antidepressant response (44). Additionally, TMS has been shown to normalize default mode network (DMN) hyperconnectivity (48). The increase in MS-2 and decreased presence of MS-3 in our TMS responders may similarly reflect this DMN recalibration. We note, however, that the controversial validity of reverse inference should be acknowledged (49, 50), and the inverse relationship of microstates 2 and 3 may reflect the constraints of microstate clustering.

We found baseline microstate features were not significantly associated with baseline clinical or demographic characteristics, including baseline depression severity. We did not have a non-depressed control sample for cross-sectional comparisons, but others (11) have found significant microstate group differences when comparing depressed individuals to controls, with significant linear relationships between depression severity and certain microstate features. Similar to EEG microstates, dynamic co-activation pattern (CAP) analyses of resting fMRI time series data also identify states with subject-level metrics such as dwell time, occurrence, persistence, and transition. Greater dynamic presence of frontoinsular-default network states (involving regions identified in our EEG data as microstates 2 and 3) was associated with more severe depression in an adolescent patient sample (51).

Critical next steps include investigating the progression of these microstate changes over the course of treatment to understand how they evolve. If microstate changes like those we measured could be detected upon initial interrogation with a specific TMS protocol or in advance of weeks of daily sessions required for symptom resolution, then perhaps EEG microstate analysis could be harnessed for providing feedback to inform clinical decision making on an individual patient level. However, determining whether the microstate changes we observed are specific to TMS, or to other brain stimulation therapies, is an important question for determining their potential clinical utility. Similar to our findings, successful seizure therapy delivered either as electroconvulsive therapy or as magnetic seizure therapy was found to correlate with a decrease in canonical microstate D frequency, subjectively similar to MS-3 (14), arguing against specificity for TMS. Additionally, microstate metrics comparing pre-treatment baseline and after two weeks of escitalopram were not associated with differential treatment outcomes (42), but that investigation did not analyze within-

subject microstate changes over time in relation to clinical response to the antidepressant. Taken together, the current study adds to the evidence base that distinct depression networks are therapeutically altered in those who respond to antidepressant treatment and not altered in those who don't. This is a step towards better understanding the network associated deficits involved in depression and how they can be modulated in TMS therapy.

To place our findings in context with other relevant research, we note that previously published microstate studies evaluated samples of unipolar, mostly unmedicated depressed patients (11) or mixed unipolar and bipolar subjects (40, 52). Owing to insurance coverage criteria, the patients in our sample had at least moderately-severe unipolar depression resistant to pharmacotherapy. Most of our patients continued on multiple psychotropic medications, including antidepressant agents, during their courses of TMS. While it has not been specifically investigated, the use of psychotropic medications may impact microstates associated with specific patterns (53). While representing an important subset of the general depression patient population, the characteristics of our naturalistically treated sample may limit comparisons of the current findings to those previously reported.

Some limitations should also be noted in the interpretation of our findings. Microstate segmentation has drawn criticism as an overly simplistic measure of EEG dynamics. The "winner-take-all" labeling excludes the possibility of competing microstate classes during EEG segments and presumes discontinuous EEG evolution (54). Although these EEG features appear to reflect a clinically relevant measure, we were careful to interpret results of our microstate analysis within the constraints of its GEV (76.5%) and clustering methods, and the approach we used generated results accounting for a large amount of the variance in brain activity. We also note the stringency of our cleaning and artifact identification methods as a possible limitation. Due to the number of recordings and the nature of microstate analysis, we utilized largely automated cleaning methods with rigorous artifact rejection, at the possible expense of eliminating true neural signal. Similarly, interpretations of sLORETA localization are limited by the low spatial resolution of the inverse solution and by using a template MRI for all subjects' forward solution. Despite the lack of precision inherent in this method, using source localization was useful to speculate about possible mechanistic underpinnings for our microstate results.

The naturalistic design of this study precluded a sham control group. Consequently, our findings may simply reflect a more general antidepressant response, subject to placebo confounds, rather than neuromodulation-induced changes. Concurrent medication use, length of current episode, and motor threshold were not assessed as possible covariates affecting microstate change, and future work should investigate these potential effects.

Analysis of EEG microstates is a nascent field and still focused largely on signal detection; standards for correction of significance thresholds in the face of multiple comparisons with several metrics for each microstate are lacking. We attempted to apply the same analysis strategy and correction factors used by Murphy and colleagues (11) to promote consistency and comparison across reports, but more replication efforts using additional databases across multiple research groups will be helpful for interpretation of these results. As previously noted, the significance thresholds for correlation tests between changes in microstate metrics

and depression score changes are uncorrected and should be interpreted as such. Finally, since the coverage metric is dependent on both duration and occurrence, findings that we and others report about changes in microstate coverage might simply be a product of the occurrence factor. Additional work is needed to evaluate whether coverage is an important or meaningful independent metric of microstates.

Follow-up steps should evaluate the underlying functional connectivity of individual microstates. While each state is believed to represent a global network, average source activation, as presented here, is not a robust EEG connectivity metric. Coherence, phase-amplitude coupling, and orthogonalized envelope correlation in source space would more accurately quantify functional connectivity and possibly reveal stronger EEG biomarkers descriptive of TMS response. Of particular interest will be future studies comparing static and dynamic network activity, measured by either EEG or fMRI or both, in a longitudinal fashion as patients progress through various states of symptom severity and remission.

In summary, these results are the first to describe a novel modulation of temporal dynamics in antidepressant response to a standard course of TMS therapy. Numerous prior investigations have utilized fMRI and EEG static spectral-power values in the context of TMS, but here our microstate analysis quantifies temporally distinct aspects of resting-state networks, unobservable at the slow fMRI timescale, and representative of global dynamics lost in time-frequency decomposition. Our results generally replicated findings reported from a depressed sample receiving other (non-TMS) types of neuromodulation therapies, i.e, a decrease in occurrence of a microstate similar in topography and localization to our MS-3 (14). Taken together, these neuromodulation-induced microstate changes may suggest a shared teleologic antidepressant mechanism.

Supplementary Material

Refer to Web version on PubMed Central for supplementary material.

Acknowledgements

The authors thank Butler Hospital clinical staff, K. Audette and A. Logan, for their collaboration with researchers and TMS clinical service. We additionally thank A. P. Gobin for database assistance.

Funding

Research was facilitated by the National Institute of General Medical Sciences of the National Institutes of Health under Award Number P20GM130452, Center for Biomedical Research Excellence, Center for Neuromodulation. The content is solely the responsibility of the authors and does not represent the official views of the National Institutes of Health. Additional funding support was provided from the Carney Institute of Brain Science and the Norman Prince Neurosciences Institute.

Conflicts of Interest

Dr. Carpenter has served as a consultant to Neuronetics Inc, Nexstim PLC, Affect Neuro Inc, Neurolief LTD, Sage Therapeutics, Otsuka, and Janssen Pharmaceuticals Inc. She has received research support (to Butler Hospital) from Neuronetics Inc, Neosync Inc, Nexstim PLC, Affect Neuro Inc, Neurolief LTD, and Janssen Pharmaceuticals Inc. Dr. Sherif has performed consulting services for In Silico Biosciences, Inc.

Bibliography

1. Eshel N, Keller CJ, Wu W, Jiang J, Mills-Finnerty C, Huemer J, et al. Global connectivity and local excitability changes underlie antidepressant effects of repetitive transcranial magnetic stimulation. Neuropsychopharmacology. 2020 2020/05/01;45(6):1018–25. [PubMed: 32053828]
2. Philip NS, Barredo J, van't Wout-Frank M, Tyrka AR, Price LH, Carpenter LL. Network mechanisms of clinical response to transcranial magnetic stimulation in posttraumatic stress disorder and major depressive disorder. Biological psychiatry. 2018;83(3):263–72. [PubMed: 28886760]
3. Thut G, Schyns P, Gross J. Entrainment of perceptually relevant brain oscillations by non-invasive rhythmic stimulation of the human brain. Frontiers in psychology. 2011;2:170. [PubMed: 21811485]
4. Corlier J, Carpenter LL, Wilson AC, Tirrell E, Gobin AP, Kavanaugh B, et al. The relationship between individual alpha peak frequency and clinical outcome with repetitive Transcranial Magnetic Stimulation (rTMS) treatment of Major Depressive Disorder (MDD). Brain stimulation. 2019;12(6):1572–8. [PubMed: 31378603]
5. Roelofs CL, Krepel N, Corlier J, Carpenter LL, Fitzgerald PB, Daskalakis ZJ, et al. Individual alpha frequency proximity associated with repetitive transcranial magnetic stimulation outcome: An independent replication study from the ICON-DB consortium. Clinical Neurophysiology. 2021;132(2):643–9. [PubMed: 33243617]
6. Carpenter LL, Janicak PG, Aaronson ST, Boyadjis T, Brock DG, Cook IA, et al. TRANSCRANIAL MAGNETIC STIMULATION (TMS) FOR MAJOR DEPRESSION: A MULTISITE, NATURALISTIC, OBSERVATIONAL STUDY OF ACUTE TREATMENT OUTCOMES IN CLINICAL PRACTICE. Depression and Anxiety. 2012 2012/07/01;29(7):587–96. [PubMed: 22689344]
7. Drysdale AT, Grosenick L, Downar J, Dunlop K, Mansouri F, Meng Y, et al. Resting-state connectivity biomarkers define neurophysiological subtypes of depression. Nature medicine. 2017;23(1):28–38.
8. Zhang Y, Wu W, Toll RT, Naparstek S, Maron-Katz A, Watts M, et al. Identification of psychiatric disorder subtypes from functional connectivity patterns in resting-state electroencephalography. Nature Biomedical Engineering. 2020:1–15.
9. Wu W, Zhang Y, Jiang J, Lucas MV, Fonzo GA, Rolle CE, et al. An electroencephalographic signature predicts antidepressant response in major depression. Nature Biotechnology. 2020 2020/02/10.
10. Corlier J, Wilson A, Hunter AM, Vince-Cruz N, Krantz D, Levitt J, et al. Changes in Functional Connectivity Predict Outcome of Repetitive Transcranial Magnetic Stimulation Treatment of Major Depressive Disorder. Cerebral Cortex. 2019.
11. Murphy M, Whitton AE, Deccy S, Ironside ML, Rutherford A, Beltzer M, et al. Abnormalities in electroencephalographic microstates are state and trait markers of major depressive disorder. Neuropsychopharmacology. 2020;45(12):2030–7. [PubMed: 32590838]
12. Michel CM, Koenig T. EEG microstates as a tool for studying the temporal dynamics of whole-brain neuronal networks: a review. Neuroimage. 2018;180:577–93. [PubMed: 29196270]
13. Yan D, Liu J, Liao M, Liu B, Wu S, Li X, et al. Prediction of Clinical Outcomes With EEG Microstate in Patients With Major Depressive Disorder. Frontiers in Psychiatry. 2021 2021-August-16;12(1386). English.
14. Atluri S, Wong W, Moreno S, Blumberger DM, Daskalakis ZJ, Farzan F. Selective modulation of brain network dynamics by seizure therapy in treatment-resistant depression. NeuroImage: Clinical. 2018;20:1176–90. [PubMed: 30388600]
15. Pan Z, Xiong D, Xiao H, Li J, Huang Y, Zhou J, et al. The Effects of Repetitive Transcranial Magnetic Stimulation in Patients with Chronic Schizophrenia: Insights from EEG Microstates. Psychiatry Research. 2021;299:113866.
16. Diagnostic and statistical manual of mental disorders : DSM-5: Fifth edition. Arlington, VA : American Psychiatric Association, [2013]; 2013.

17. Perera T, George MS, Grammer G, Janicak PG, Pascual-Leone A, Wirecki TS. The Clinical TMS Society Consensus Review and Treatment Recommendations for TMS Therapy for Major Depressive Disorder. Brain Stimul. 2016 May-Jun;9(3):336–46. PubMed PMID: 27090022. PMCID: PMC5612370. Epub 2016/04/20. eng. [PubMed: 27090022]
18. McClintock SM, Reti IM, Carpenter LL, McDonald WM, Dubin M, Taylor SF, et al. Consensus Recommendations for the Clinical Application of Repetitive Transcranial Magnetic Stimulation (rTMS) in the Treatment of Depression. J Clin Psychiatry. 2018 Jan/Feb;79(1). PubMed PMID: 28541649. PMCID: PMC5846193. Epub 2017/05/26. eng.
19. Rush AJ, Gullion CM, Basco MR, Jarrett RB, Trivedi MH. The Inventory of Depressive Symptomatology (IDS): psychometric properties. Psychological Medicine. 1996;26(3):477–86. Epub 2009/07/09. [PubMed: 8733206]
20. Harrell Jr FE, Slaughter JC. Introduction to biostatistics for biomedical research. URL: http://hbiostatorg/doc/bbrpdf Last visited: September. 2001;2:2019.
21. Nilsonne G, Harrell FE. EEG-based model and antidepressant response. Nature Biotechnology. 2021 2021/01/01;39(1):27-.
22. Wu W, Pizzagall DA, Trivedi MH, Etkin A. Reply to: EEG-based model and antidepressant response. Nature Biotechnology. 2021 2021/01/01;39(1):28–9.
23. Delorme A, Makeig S. EEGLAB: an open source toolbox for analysis of single-trial EEG dynamics including independent component analysis. Journal of neuroscience methods. 2004;134(1):9–21. [PubMed: 15102499]
24. Perrin F, Pernier J, Bertnard O, Giard M-H, Echallier J. Mapping of scalp potentials by surface spline interpolation. Electroencephalography and clinical neurophysiology. 1987;66(1):75–81. [PubMed: 2431869]
25. de Cheveigné A ZapLine: A simple and effective method to remove power line artifacts. Neuroimage. 2020;207:116356.
26. Palmer JA, Makeig S, Kreutz-Delgado K, Rao BD, editors. Newton method for the ICA mixture model. 2008 IEEE International Conference on Acoustics, Speech and Signal Processing; 2008: IEEE.
27. Acar ZA, Makeig S. Neuroelectromagnetic forward head modeling toolbox. Journal of neuroscience methods. 2010;190(2):258–70. [PubMed: 20457183]
28. Pion-Tonachini L, Kreutz-Delgado K, Makeig S. ICLabel: An automated electroencephalographic independent component classifier, dataset, and website. NeuroImage. 2019;198:181–97. [PubMed: 31103785]
29. Artoni F, Menicucci D, Delorme A, Makeig S, Micera S. RELICA: a method for estimating the reliability of independent components. Neuroimage. 2014;103:391–400. [PubMed: 25234117]
30. Poulsen AT, Pedroni A, Langer N, Hansen LK. Microstate EEGlab toolbox: An introductory guide. BioRxiv. 2018 (289850).
31. Khanna A, Pascual-Leone A, Farzan F. Reliability of resting-state microstate features in electroencephalography. PloS one. 2014;9(12):e114163.
32. Pascual-Marqui RD, Michel CM, Lehmann D. Segmentation of brain electrical activity into microstates: model estimation and validation. IEEE Transactions on Biomedical Engineering. 1995;42(7):658–65. [PubMed: 7622149]
33. Krzanowski WJ, Lai Y. A criterion for determining the number of groups in a data set using sum-of-squares clustering. Biometrics. 1988:23–34.
34. Tadel F, Baillet S, Mosher JC, Pantazis D, Leahy RM. Brainstorm: a user-friendly application for MEG/EEG analysis. Computational intelligence and neuroscience. 2011;2011.
35. Gramfort A, Papadopoulo T, Olivi E, Clerc M. OpenMEEG: opensource software for quasistatic bioelectromagnetics. Biomedical engineering online. 2010;9(1):1–20.
36. Pascual-Marqui RD. Standardized low-resolution brain electromagnetic tomography (sLORETA): technical details. Methods Find Exp Clin Pharmacol. 2002;24(Suppl D):5–12. [PubMed: 12575463]
37. Friston KJ, Holmes AP, Price C, Büchel C, Worsley K. Multisubject fMRI studies and conjunction analyses. Neuroimage. 1999;10(4):385–96. [PubMed: 10493897]

38. Philip NS, Barredo J, Aiken E, Carpenter LL. Neuroimaging Mechanisms of Therapeutic Transcranial Magnetic Stimulation for Major Depressive Disorder. Biological Psychiatry: Cognitive Neuroscience and Neuroimaging. 2018;3(3):211–22. en. [PubMed: 29486862]
39. Britz J, Van De Ville D, Michel CM. BOLD correlates of EEG topography reveal rapid resting-state network dynamics. Neuroimage. 2010;52(4):1162–70. [PubMed: 20188188]
40. Damborská A, Tomescu MI, Honzírková E, Barteček R, Hořínková J, Fedorová S, et al. EEG resting-state large-scale brain network dynamics are related to depressive symptoms. Frontiers in psychiatry. 2019;10:548. [PubMed: 31474881]
41. Siddiqi SH, Taylor SF, Cooke D, Pascual-Leone A, George MS, Fox MD. Distinct symptom-specific treatment targets for circuit-based neuromodulation. American Journal of Psychiatry. 2020;177(5):435–46.
42. Zhdanov A, Atluri S, Wong W, Vaghei Y, Daskalakis ZJ, Blumberger DM, et al. Use of Machine Learning for Predicting Escitalopram Treatment Outcome From Electroencephalography Recordings in Adult Patients With Depression. JAMA network open. 2020;3(1):e1918377-e. PubMed PMID: 31899530. eng.
43. Williams LM. Defining biotypes for depression and anxiety based on large-scale circuit dysfunction: a theoretical review of the evidence and future directions for clinical translation. Depress Anxiety. 2017 Jan;34(1):9–24. PubMed PMID: 27653321. PMCID: PMC5702265. Epub 2016/10/21. eng. [PubMed: 27653321]
44. Kaiser RH, Andrews-Hanna JR, Wager TD, Pizzagalli DA. Large-Scale Network Dysfunction in Major Depressive Disorder: A Meta-analysis of Resting-State Functional Connectivity. JAMA Psychiatry. 2015;72(6):603–11. [PubMed: 25785575]
45. Zhang J, Wang J, Wu Q, Kuang W, Huang X, He Y, et al. Disrupted brain connectivity networks in drug-naive, first-episode major depressive disorder. Biol Psychiatry. 2011 Aug 15;70(4):334–42. PubMed PMID: 21791259. Epub 2011/07/28. eng. [PubMed: 21791259]
46. Fox MD, Liu H, Pascual-Leone A. Identification of reproducible individualized targets for treatment of depression with TMS based on intrinsic connectivity. Neuroimage. 2013;66:151–60. [PubMed: 23142067]
47. Fox MD, Buckner RL, White MP, Greicius MD, Pascual-Leone A. Efficacy of transcranial magnetic stimulation targets for depression is related to intrinsic functional connectivity with the subgenual cingulate. Biological psychiatry. 2012;72(7):595–603. [PubMed: 22658708]
48. Liston C, Chen AC, Zebley BD, Drysdale AT, Gordon R, Leuchter B, et al. Default mode network mechanisms of transcranial magnetic stimulation in depression. Biological psychiatry. 2014;76(7):517–26. [PubMed: 24629537]
49. Poldrack RA. Can cognitive processes be inferred from neuroimaging data? Trends in Cognitive Sciences. 2006 2006/02/01/;10(2):59–63. [PubMed: 16406760]
50. Hutzler F Reverse inference is not a fallacy per se: Cognitive processes can be inferred from functional imaging data. NeuroImage. 2014 2014/01/01/;84:1061–9. [PubMed: 23313571]
51. Kaiser RH, Kang MS, Lew Y, Van Der Feen J, Aguirre B, Clegg R, et al. Abnormal frontoinsular-default network dynamics in adolescent depression and rumination: a preliminary resting-state co-activation pattern analysis. Neuropsychopharmacology. 2019 2019/08/01;44(9):1604–12. [PubMed: 31035283]
52. Strik W, Dierks T, Becker T, Lehmann D. Larger topographical variance and decreased duration of brain electric microstates in depression. Journal of Neural Transmission/General Section JNT. 1995;99(1–3):213–22.
53. Mackintosh AJ, Borgwardt S, Studerus E, Riecher-Rössler A, de Bock R, Andreou C. EEG Microstate Differences in Medicated vs. Medication-Naïve First-Episode Psychosis Patients. Frontiers in Psychiatry. 2020 2020-November-24;11(1320). English.
54. Shaw SB, Dhindsa K, Reilly JP, Becker S. Capturing the Forest but Missing the Trees: Microstates Inadequate for Characterizing Shorter-Scale EEG Dynamics. Neural computation. 2019;31(11):2177–211. [PubMed: 31525310]

HIGHLIGHTS

- EEG microstates are believed to represent transient activations of global networks
- Distinct microstate networks changed in clinical response to TMS
- These changes may reflect default-mode network recalibration in antidepressant response

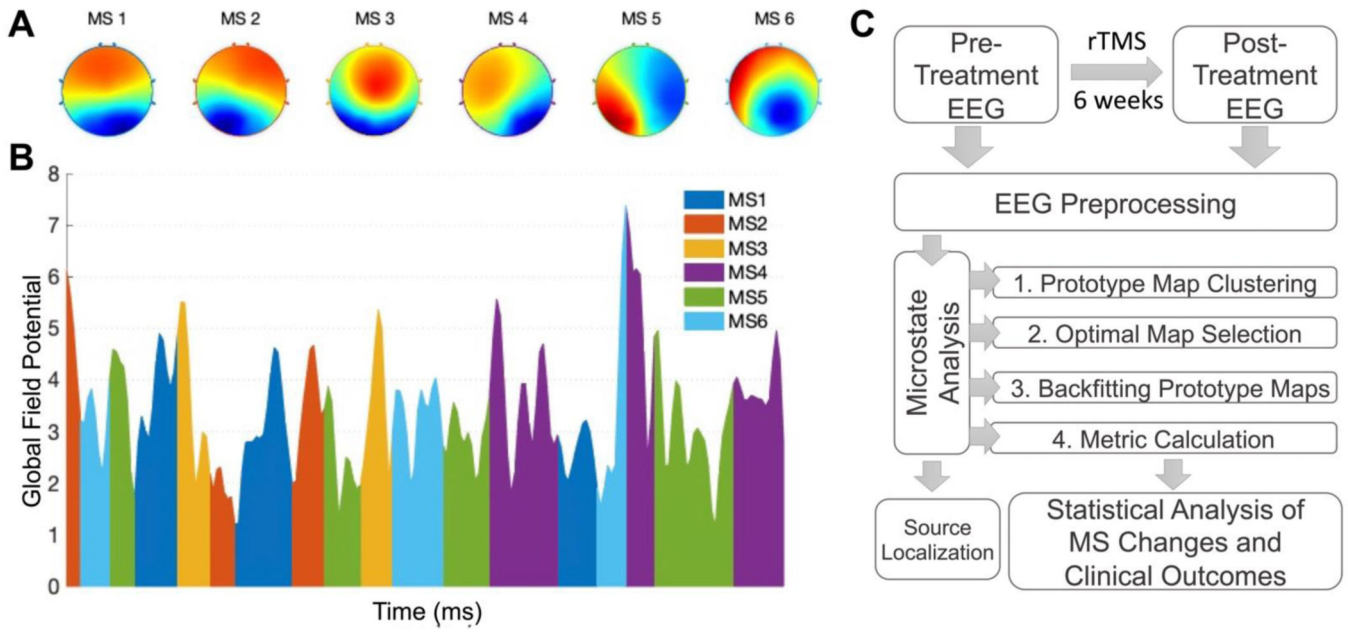

Figure 1. Microstate Topographies, Representation, and Study Pipeline.

A) 6 clustered prototype microstate voltage maps. B) Representative sample from one subject over a 1 second microstate segmentation of EEG transformed into its Global Field Potential (GFP). K-means clustering utilizes the EEG signal at GFP peaks. C) Analysis flowchart. Microstate identification analysis clustered all available recordings, and subsequent formal analyses were conducted on a subset of patients with a complete set of recordings and clinical outcomes. Source localization utilized only pre-treatment recordings.

2a

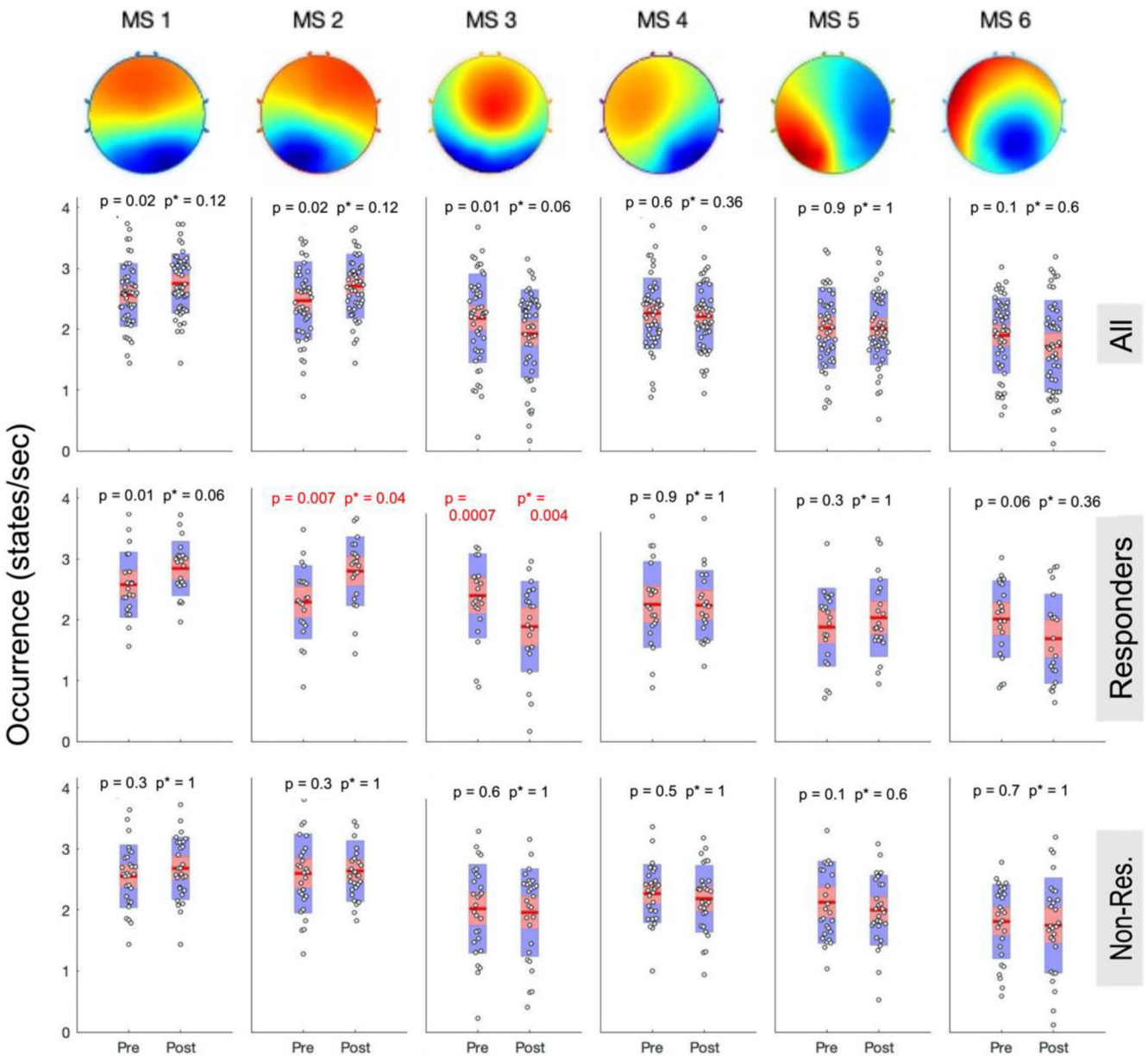

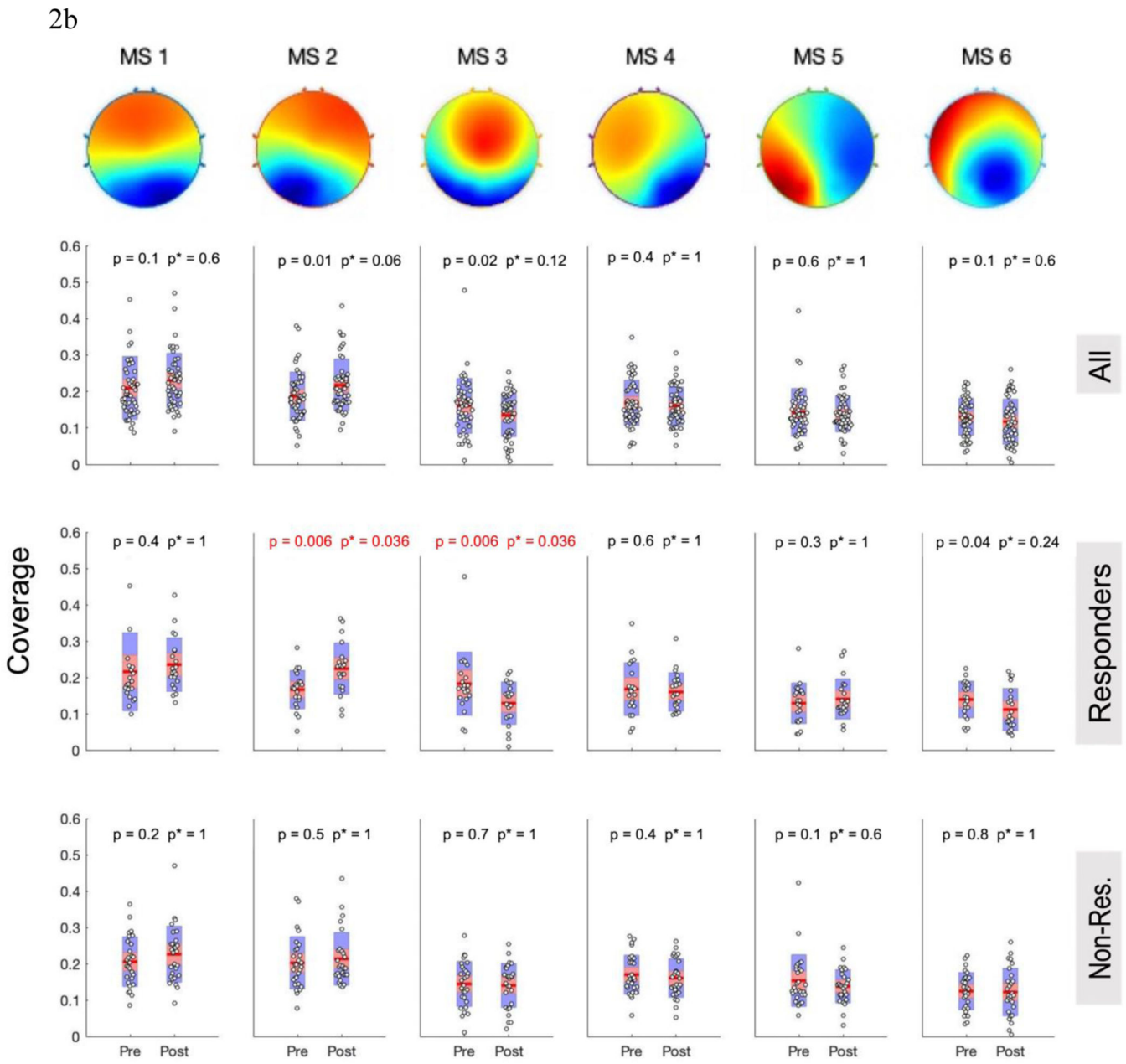

Figure 2: Categorical Microstate Changes After TMS Course.

A) Occurrence and B) Coverage of MS-1 – 6 (left to right) for the all subjects together (top row), responders (middle row), and non-responders (bottom row). Red p-values meet the Bonferroni-corrected significance threshold (p<0.0083); uncorrected p-values are displayed on left, followed by corrected p*-values on right. Red line is the mean, red bar displays the standard error of the mean, and blue bar displays the standard deviation

a.

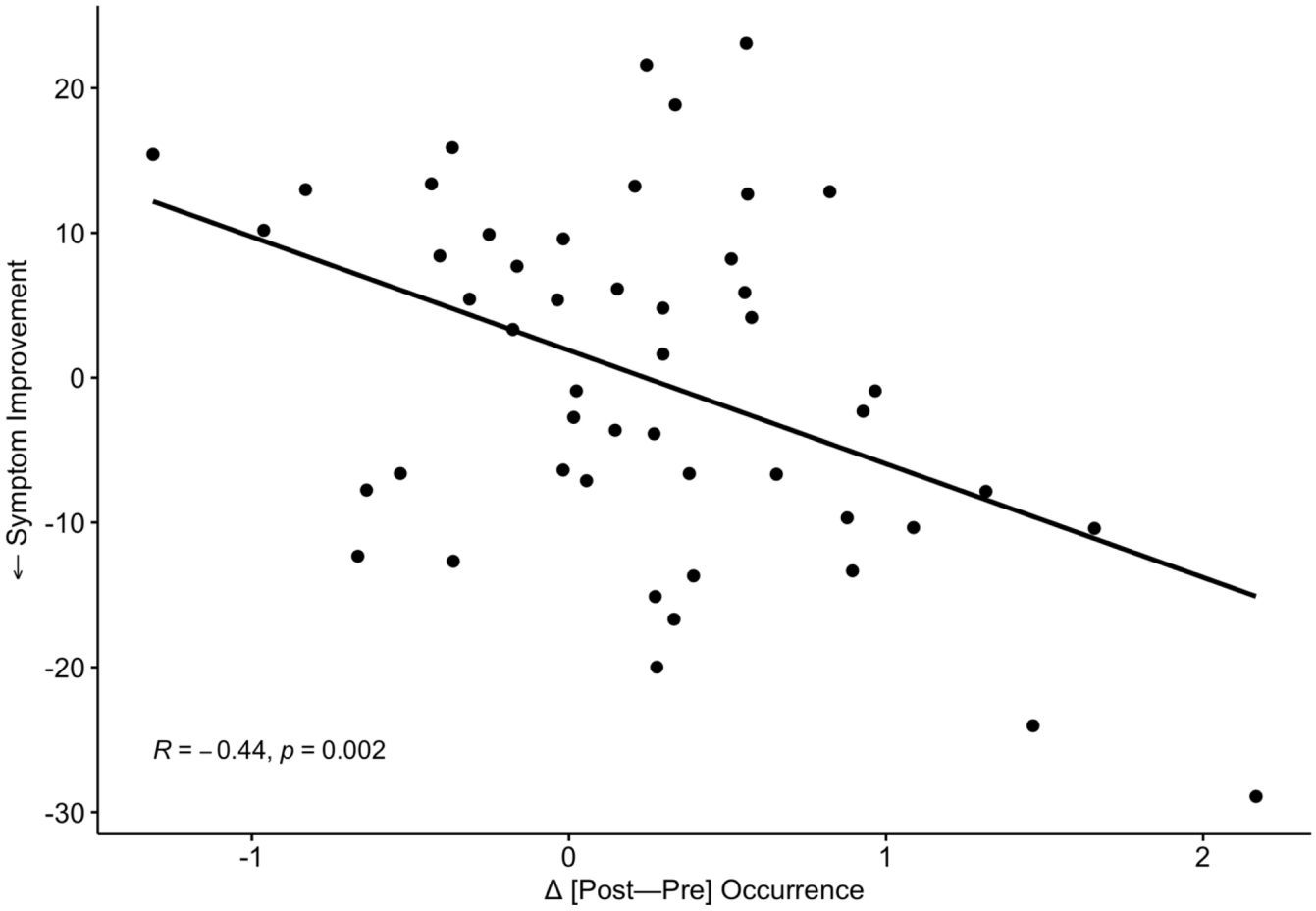

b.

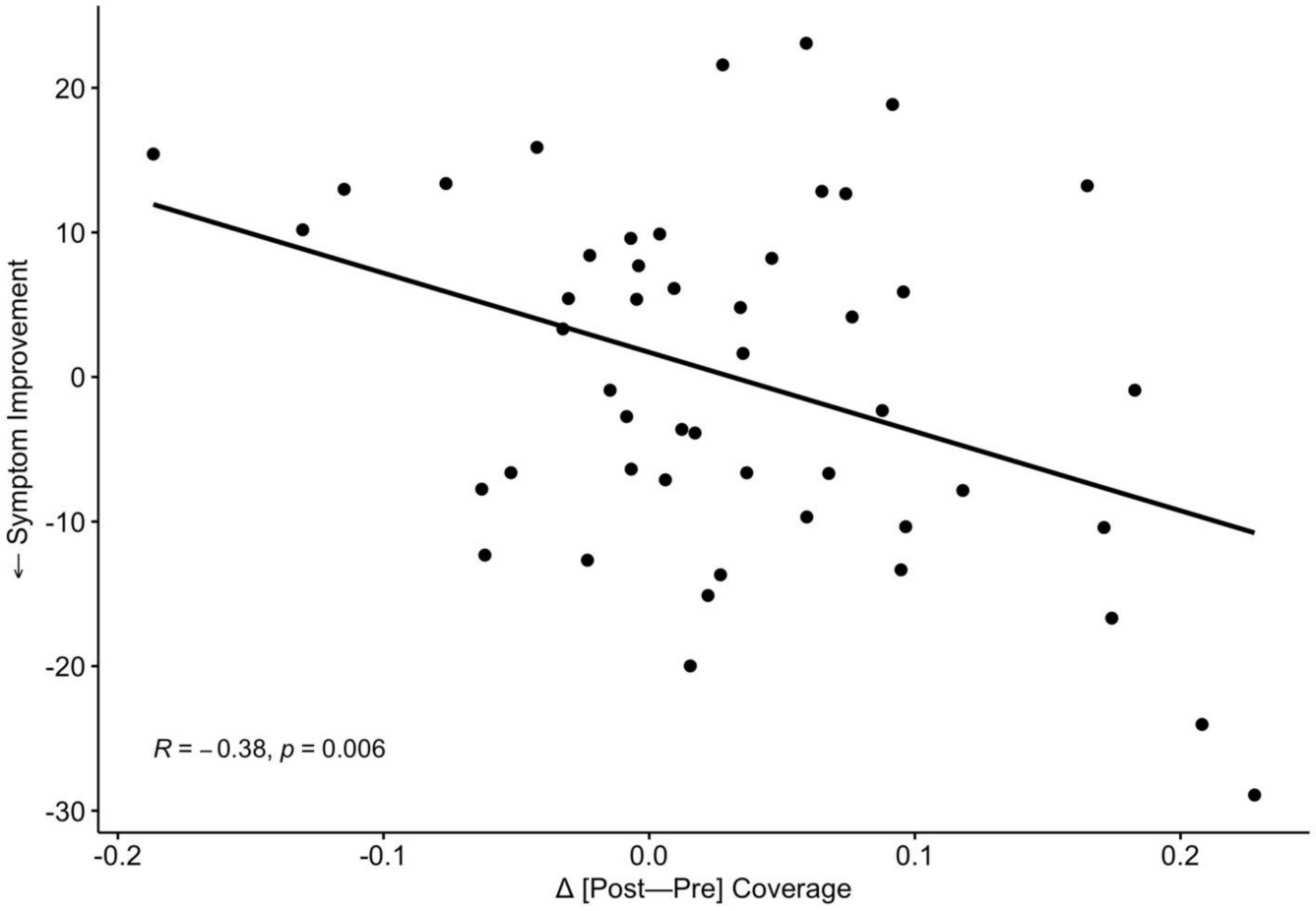

c.

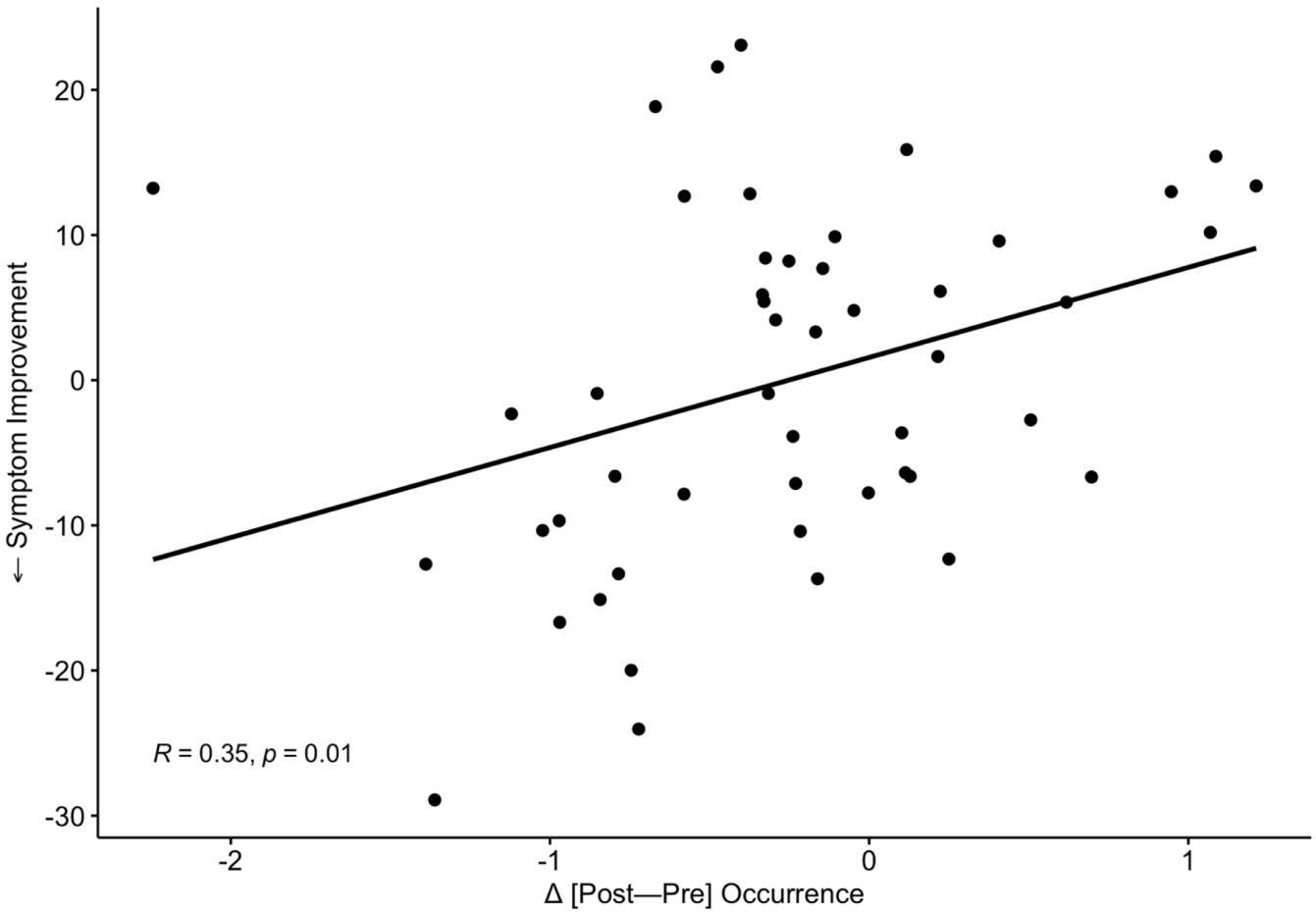

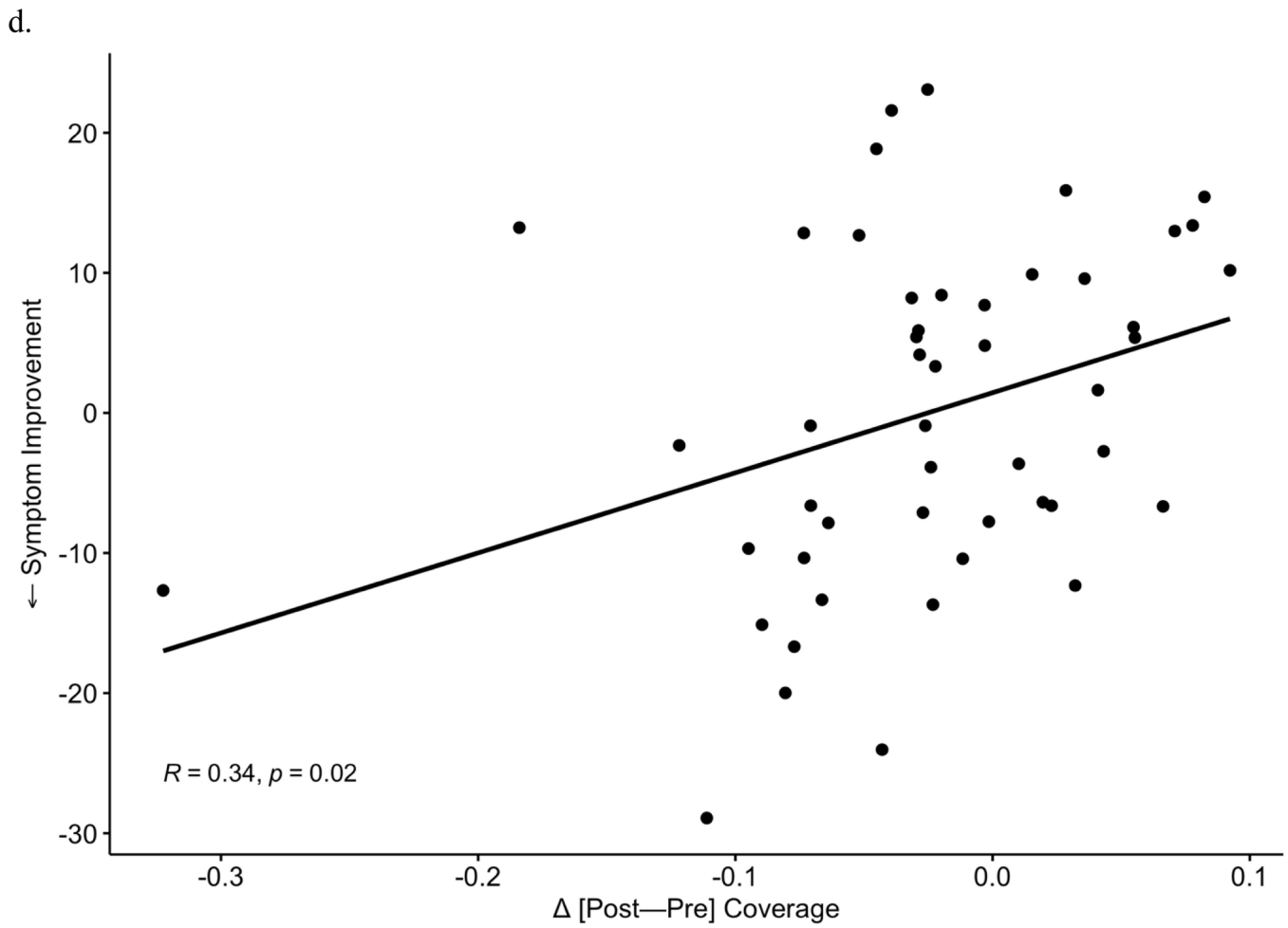

Figure 3: Symptom Correlation with Microstates Change.

Increases in occurrence (a) and coverage (b) of MS 2 significantly correlate with improvements in depressive symptoms. Reciprocally, decreases in MS 3 occurrence (c) and coverage (d) correlate with symptom improvement.

4a MS-**2**

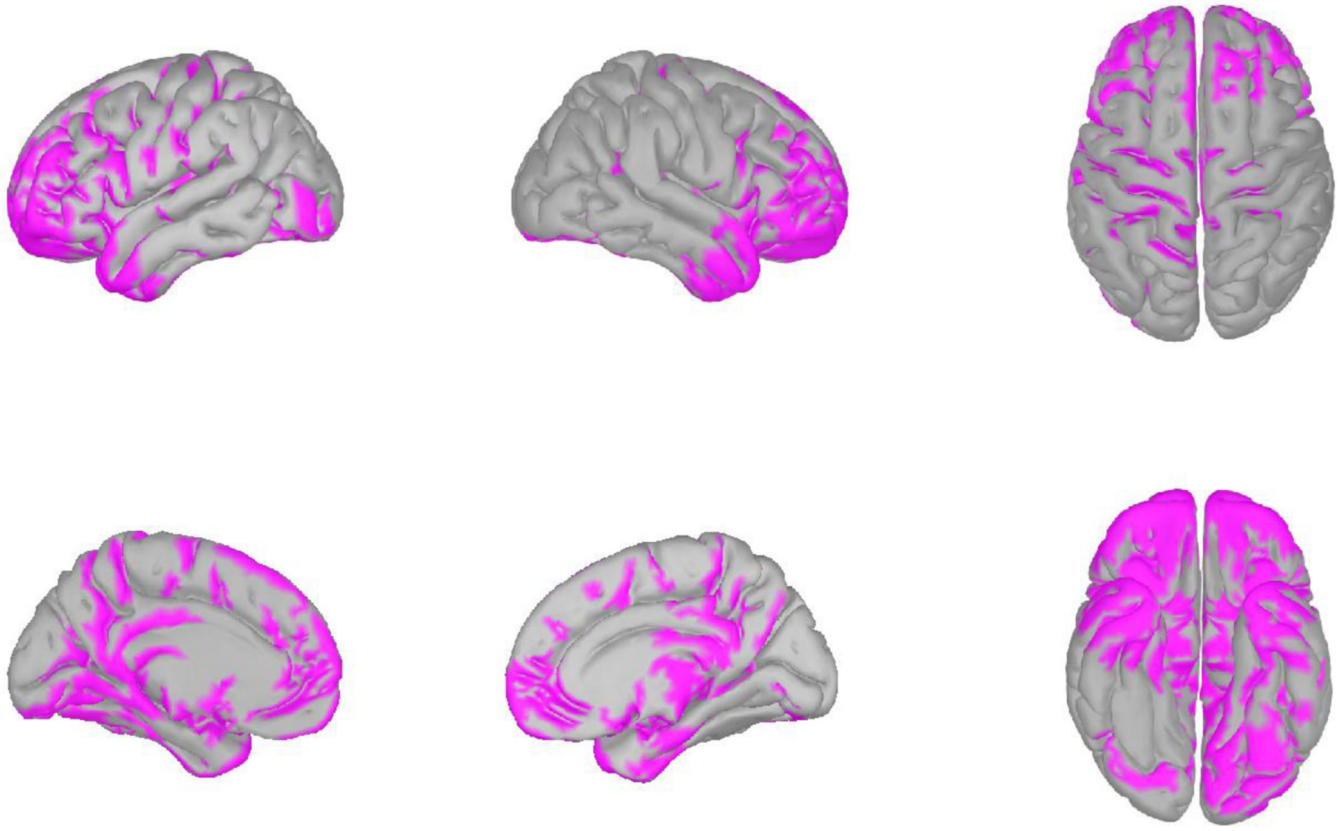

4b MS-**3**

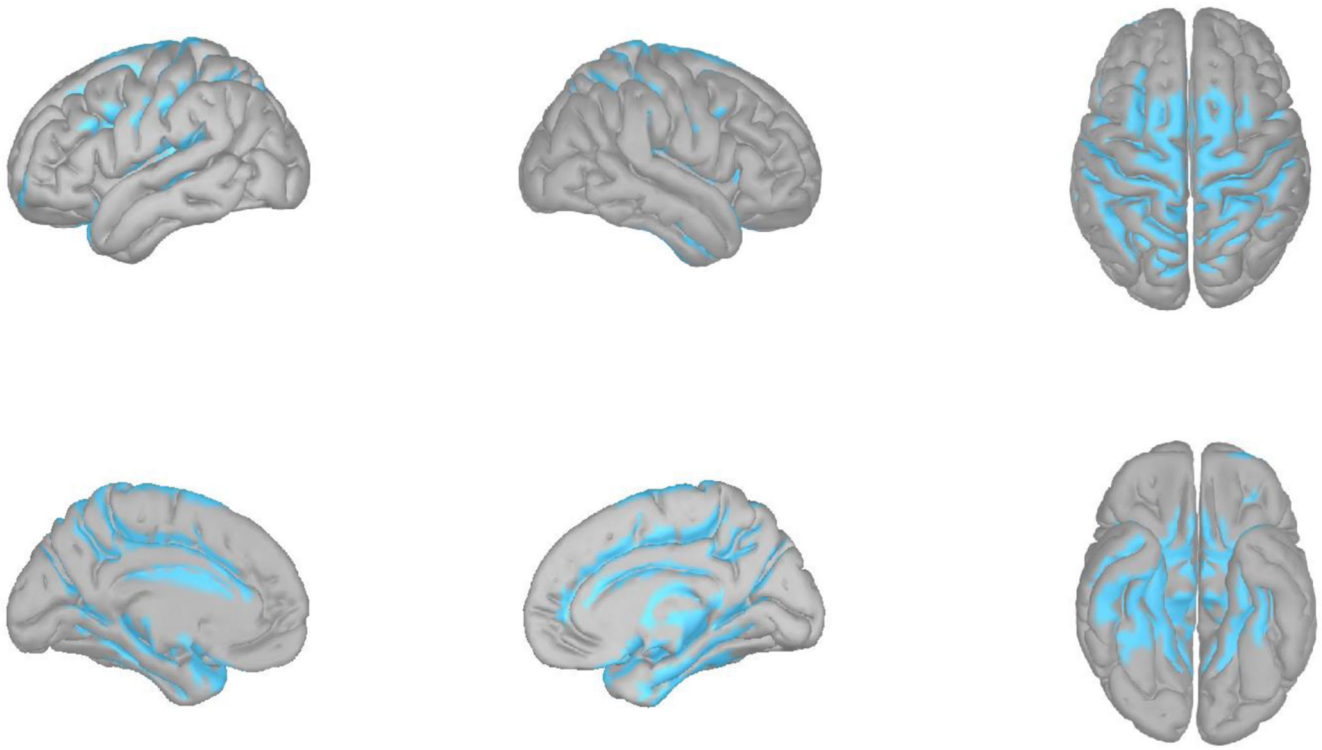

Figure 4: Source Localization for MS2 and MS3.
sLORETA average activations of MS 2 (a), MS 3 (b).

Table 1.

Demographic, Clinical, and Treatment Characteristics (N=49)

	Range or N	Mean (SD) or %
Baseline Depression Severity (IDS-SR total)	29 – 82	49 (11)
Age (years)	20 – 77	44 (15)
Sex (Female)	32	65%
Past (Lifetime) ECT	11	22%
Past (Lifetime) Psychiatric Hospitalization	29	59%
Past TMS Therapy (Prior Depressive Episode)	12	25%
Total Number of TMS (Current Episode)	33 – 46	36 (2)